



Enhancing power generation of scale-up microbial fuel cells by optimizing the leading-out terminal of anode



Shaoan Cheng*, Yaoli Ye, Weijun Ding, Bin Pan

State Key Laboratory of Clean Energy Utilization, Department of Energy Engineering, Zhejiang University, Hangzhou 310027, PR China

HIGHLIGHTS

- A simple model to simulate the power loss of scale up microbial fuel cell.
- Leading-out terminal could result in more than 47.1% of power loss.
- Leading-out terminal of anode is one of the key factors for scaling up MFC.

ARTICLE INFO

Article history:

Received 23 June 2013

Received in revised form

2 October 2013

Accepted 7 October 2013

Available online 15 October 2013

Keywords:

Microbial fuel cells

Scale-up

Simulation

Leading-out terminal

Inferior anode

ABSTRACT

Low power output and high cost are two major challenges for scaling up microbial fuel cell (MFC). The ohmic resistance of anode increasing as MFCs scale up can be one of main reasons for power density decrease. We present a simple model to simulate power loss and potential drop distribution caused by ohmic resistance of carbon mesh anodes with different dimensions and various leading-out terminals. We also conduct experiments to confirm the simulation work and the large impact of anode ohmic resistance on large-scale MFCs by varying leading-out configurations. The simulation results show that the power loss with an anode size of 1 m² can be as high as 4.19 W at current density of 3 A m⁻², and the power loss can be decreased to 0.04 W with optimized configuration of leading-out terminals and to 0.01 W by utilizing brass mesh as anode material. The experiments well confirm the simulation results with the deviations less than 11.0%. Furthermore, the experiment results also show that more than 47.1% of the power loss from small-scale to large-scale MFC comes from bad-leading-out terminal. These results demonstrate that leading-out terminal of anode is one of the key factors for scaling up MFC.

© 2013 Elsevier B.V. All rights reserved.

1. Introduction

Microbial fuel cells are devices that generate electricity from oxidation of organic compounds with microbes as catalyst. MFC holds great potential to become a sustainable way of extracting energy from wastewater and doing wastewater treatment simultaneously. Different configurations of MFCs have been tested, such as tubular [1], flat plate [2], upflow [3], downflow [4], two-chamber and single-chamber [5], cloth electrode assemblies (CEA) [6] and spiral wound [7]. In all variety of configurations, single-chamber air-cathode MFCs may be the fittest candidate for scaling up for its relatively low cost, simple and compact structure, and high power output. The carbon based materials, with qualities as conductivity, biocompatibility and chemical stability, are mostly used as anode in MFC, such as carbon cloth [8], carbon fiber felt [9], carbon fiber brush [10], carbon mesh

[11]. However, carbon cloth and carbon felt have relatively high cost, and may not suit for scale-up MFC. Carbon brush has low cost and high surface area, but it is unable to be used to construct a compact structure for high volumetric power density of MFC. Carbon mesh, with low cost and showing good performance in compact MFCs, could be an alternative anode material for scale-up MFC. Aside from carbon mesh, metal mesh is another alternative to be anode material for its super conductivity, but metal mesh has low surface area and bad biocompatibility [12]. Up to now, in laboratory scale (less than 30 mL), the maximum area power density of MFCs (power normalized to the electrode surface area) has reached 6860 mW m⁻² (2.62 mA cm⁻², 12 mL) through adjustment of cathode/anode area ratio [8]; the maximum volumetric power density (power normalized to the volume) of 1.55 kW m⁻³ (0.99 mA cm⁻², 2.5 mL) has been achieved by reducing electrode spacing in pH9 bicarbonate buffer [13]. The power density achieved in small-scale MFCs under optimized conditions indicates that it is feasible to scale up MFC for practical application in terms of power generation if the power density can be maintained.

* Corresponding author. Tel.: +86 571 87952038; fax: +86 571 87951616.

E-mail address: shaaoancheng@zju.edu.cn (S. Cheng).

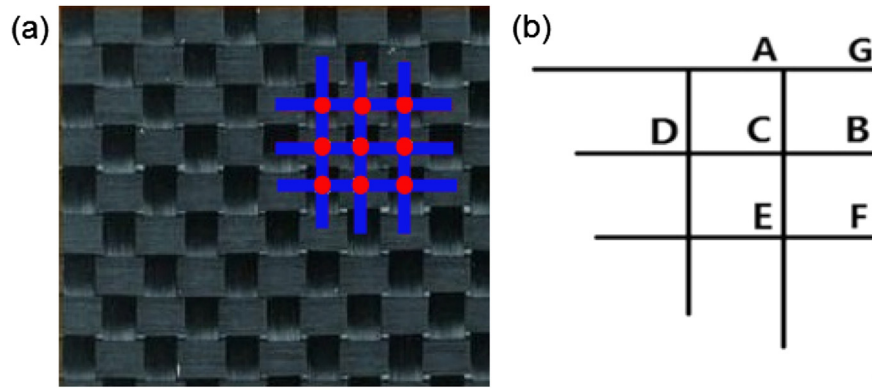


Fig. 1. A photograph of carbon mesh (a); simplified model for calculation (b).

There are two main approaches for scaling up MFC: increasing individual dimension of each cell and connecting several MFCs to form a stack system [14]. High performance of large-dimension MFCs is the prerequisite of high power-output stack system. Several investigations on large-scale MFC have been done. The single-chamber air-cathode MFC with a size of 520 mL was constructed and its volumetric power density was reported as 16 W m^{-3} [15]. The area power density reached 30 mW m^{-2} in the down-flow single-chamber MFC with a size of 850 mL [4] and 72 mW m^{-2} in a baffled MFC with volume of 1.5 L [16]. These results illustrate that scale-up MFCs perform much lower power density than small-scale MFCs, indicating that some factors certainly constrain the power output of scale-up MFCs. It has been found that power generation of MFCs is affected by pH, dissolved oxygen concentration, temperature, electrolyte, and species of bacteria resulting in the existence of ohmic, activation, concentration losses [17]. These factors had been well investigated in small-scale reactors [18–20] but less studied in scale-up MFCs. Cheng and Logan studied four MFCs with different sizes (28 mL, 250 mL, 1 L, 1.6 L) and found that anode performance was mainly affected by substrate concentration, while cathode performance was controlled by solution conductivity. They also explicitly pointed out that cathode specific area was the critical factor for high power density of scale-up MFCs [21]. The power density logarithmically decreased as the electrode size increased from 1.92 cm^2 to 155 cm^2 , which indicated that power density generated by large-electrode MFCs could not be estimated by small-electrode MFCs [22]. Different from those results, recently Fan et al. reported a maximum volumetric power density of 2.87 kW m^{-3} (4.30 W m^{-2} , 16.4 A m^{-2}) with an effective anode surface area of 200 cm^2 by using double cloth-electrode-assemblies and u-shape current collector [23]. This volumetric power density is even higher than that of small-scale MFC (anode size 14 cm^2) [13]. This result may indicate that the leading-out terminals could be one of the critical factors for high power density of the scale-up MFC.

As anode dimension gets larger, ohmic resistance of anode becomes higher, because the distance between points where electrons generate and the leading-out terminal where current flows out of anode increases. This increase in the anode resistance may lead to a significant power loss of MFC. Thus, it is necessary to better understand this part of loss for scale-up MFC. In this paper, we setup a model to simulate the power loss and potential drop distribution on the carbon mesh anode with different configurations of leading-out terminal and various dimensions. We also conduct experiments to confirm the simulation results and to demonstrate that the leading-out terminal of anode has a critical effect on power output of large-scale MFC. The possible approaches to minimize power losses are also suggested.

2. Methods and experiment

2.1. Model and calculation

To simplify calculation, seven basic assumptions made for developing the model are that (Fig. 1(a)): 1) two paralleled adjacent bundles of carbon fiber are assumed not in touch with each other; 2) contact resistance between mutually orthogonal carbon fibers is negligible; 3) the carbon mesh has uniform physical properties; 4) bundles of carbon fiber are represented as lines with same length but width ignored; 5) microbes evenly grows on the carbon mesh anode, which results in even distribution of current input; 6) current with equal value was input only into each node; 7) potential drop at the node or nodes leading out to external circuit is set to 0. The model for calculating the potential drop of the carbon mesh was represented as the mesh (Fig. 1(b)), where A, B, C, D, E, F, G were the nodes on anode simplified with assumptions. Based on Kirchhoff's Law, the sum of currents flowing into a node is equal to the sum of currents flowing out of the node. Thus, current input of any node in the mesh can be presented as follows:

The equation of the nodes at the corner of the mesh:

$$i_G^{\text{input}} = i_G^{\text{output}} = (U_G - U_A)/R_{\text{fibre}} + (U_G - U_B)/R_{\text{fibre}} \quad (1)$$

The equation of the nodes in the edge of the mesh:

$$i_B^{\text{input}} = i_B^{\text{output}} = (U_B - U_G)/R_{\text{fibre}} + (U_B - U_F)/R_{\text{fibre}} + (U_B - U_C)/R_{\text{fibre}} \quad (2)$$

The equation of the nodes in the middle:

$$i_C^{\text{input}} = i_C^{\text{output}} = (U_C - U_A)/R_{\text{fibre}} + (U_C - U_B)/R_{\text{fibre}} + (U_C - U_E)/R_{\text{fibre}} + (U_C - U_D)/R_{\text{fibre}} \quad (3)$$

The equation of the node connecting to external circuit:

$$U = 0 \\ i_{\text{input}} = 0 \quad (4)$$

In this approach, an equation is established for each node in the mesh, where U represents potential drop of a node, i the sum of currents that flow in or out of a node and R_{fibre} the resistance between two adjacent nodes. As the number of equations equals to the amount of variables, unique solution for the potential drop of

each node can be obtained with MATLAB. The power loss for each edge of a mesh unit can be calculated according to the ohm law:

$$P_{\text{loss}} = U_{\text{difference}}^2 / R_{\text{fiber}} \quad (5)$$

where $U_{\text{difference}}$ is the potential difference between two adjacent nodes. The power loss caused by current flow on anode is expressed as the sum of the power loss of each mesh unit.

Potential drop distribution on carbon mesh anode and concomitant power loss of MFC was simulated for the anodes with various configurations of leading-out terminal and different materials. The current density of 3 A m^{-2} and the power density of 1 W m^{-2} (except as noted) were selected for the simulation because they are about the values mostly reported in the small-scale MFC [10,11]. Carbon mesh (2 mm in width for each bundle of carbon fiber, $1.16 \Omega \text{ cm}^{-1}$ in resistivity, measured), brass mesh (0.45 mm in wire diameter, 1.357 mm in aperture, $0.071 \Omega \text{ mm}^2 \text{ m}^{-1}$ in resistivity) and stainless steel mesh (0.45 mm in wire diameter, 1.357 mm in aperture, $0.73 \Omega \text{ mm}^2 \text{ m}^{-1}$ in resistivity) were studied in the paper.

2.2. MFC configuration, operation and analysis

Two flat plate single-chamber air-cathode MFCs were constructed (Fig. 2(a)) as: one consisted of one anode and single cathode (SC-MFC), the other consisted of one anode and double cathodes (DC-MFC) with the anode set between the two cathodes to minimize the effect of cathode. The anodes were carbon mesh with high porous structure (Fig. 1(a)) (3K, Toray Industries, Inc.) pretreated as previously reported [11]. The cathodes were made as previously described [24]. Both the anodes and the cathodes had surface area of 2160 cm^2 . The glass fiber separators (2 mm in thickness, ChangZhou ChangHai GFRP Product Co., Ltd.) were set on the liquid-faced side of the cathodes to avoid short circuit between the anode and the cathodes. The total liquid volume of MFC was 12 L for the SC-MFC and 13 L for the DC-MFC.

The effect of the leading-out terminal of anode on the power loss of MFC was investigated in three connecting patterns involving 5 connecting points (Fig. 2(b)). The three connecting patterns (CP) were set by connecting the anodes to external circuit at point 3 (CP-1), at points of 2, 3, 4 (CP-2), and at points of 1, 2, 3, 4, 5 (CP-3).

Then MFCs were inoculated with the effluent of a single-chamber air-cathode reactor that was operated for more than 2 years using acetate. The MFCs were started up with CP-3 mode at an external resistance of 50Ω for 4 fed cycles (around 12 days), and then operated at a resistance of 1Ω for 10 cycles to mature the biofilm on anode, both in 50 mM PBS nutrient solution containing 1 g L^{-1} acetate. 50 mM PBS nutrient solution consisted of (per liter): NH_4Cl , 0.31 g; KCl , 0.13 g; $\text{NaH}_2\text{PO}_4 \cdot 2\text{H}_2\text{O}$, 2.75 g; $\text{Na}_2\text{HPO}_4 \cdot 6\text{H}_2\text{O}$, 11.466 g, and 12.5 mL L^{-1} mineral solution [25]. In order to test the effect of leading-out terminal on power loss at the high current, the DC-MFC was tested in 150 mM PBS after the 1Ω -operation. A small-scale MFC was also constructed as described [11] to identify the power loss during scaling up, and it was inoculated and operated

for more than two months at an external resistance of 1000Ω before the power density was tested by varying resistance from 1000Ω to 100Ω . The electrode material and the electrode spacing of the small-scale MFC were the same as that in the DC-MFC or the SC-MFC. All the tests were conducted in $30 \pm 2^\circ \text{C}$.

The voltage across the external resistance was monitored at 20 min intervals using a multimeter (Aglient 34970a, USA). The power density of the SC-MFC was measured by linear sweep voltammetry (LSV) with a potentiostat (Iviumstat, Netherland) in a two-electrode setup with the anode as counter and reference electrode and the cathode as working electrode. The LSV was conducted in the potential region from 0.5 V to 0.05 V at a scan rate of 0.1 mV s^{-1} .

The polarization curve of the anode in the DC-MFC was obtained by using chronopotentiometry in a three-electrode setup in which the two cathodes were connected to counter electrode, Ag/AgCl reference electrode to reference electrode and the anode to working electrode. The current varied from 0.01 A to 0.45 A. The anode was polarized for was 20 min at each current.

3. Results

3.1. Estimation of power loss

As the anode size increased from 4.84 cm^2 to 1 m^2 , the power loss slowly increased for the anode size below 0.16 m^2 but sharply increased when the anode size was over 0.16 m^2 , while the ideal power output of MFC linearly increased with the anode size (supposing no power loss when scaling up) (Fig. 3(a)). The anode ohmic resistance increased by 287.5% from 0.16Ω to 0.46Ω when the anode size enlarged from 10 cm^2 to 1 m^2 , resulting in the power loss as high as 4.19 W at an anode size of 1 m^2 . When the anode size was over 0.25 m^2 , the estimated power loss became larger than the ideal power output, indicating that in the actual cases the current density of scale-up MFC could never reach the supposing value of 3 A m^{-2} . Therefore, the actual power output would significantly decrease as the anode size increases.

On the 1 m^2 carbon mesh anode with one point connecting to external circuit, the potential drops severely increased near the connecting point and were as high as 1.51 V on the most part of the anode (Fig. 3(b)). This was because all currents on the anode converged near the connecting point and caused considerable electric energy loss. The potential drops were larger in order of magnitude than the standard anode potential for acetate oxidation of -0.296 V (vs. NHE) based on Nernst equation [26], which indicated again the supposed current density cannot be achieved on the anode with this configuration in practical condition.

3.2. Impact of connecting patterns on power output

With one leading-out point (CP-1) the SC-MFC performed a maximum power output of $38.3 \pm 0.6 \text{ mW}$ (Fig. 4). Increasing

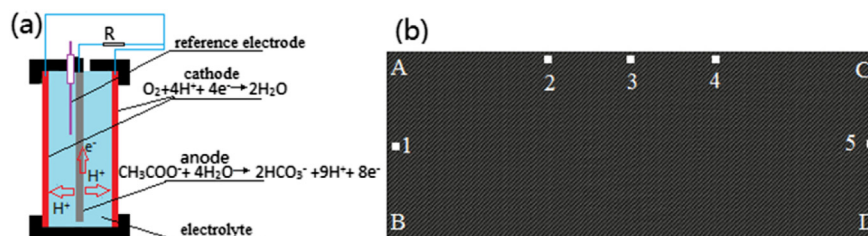


Fig. 2. The structure of the DC-MFC with two cathodes (a); connecting points on the anode: point 1 (middle point of edge AB), point 2 (1/3 in edge AC), point 3 (middle point of edge AC), point 4 (2/3 in the edge AC), point 5 (1/2 in edge CD) (b).

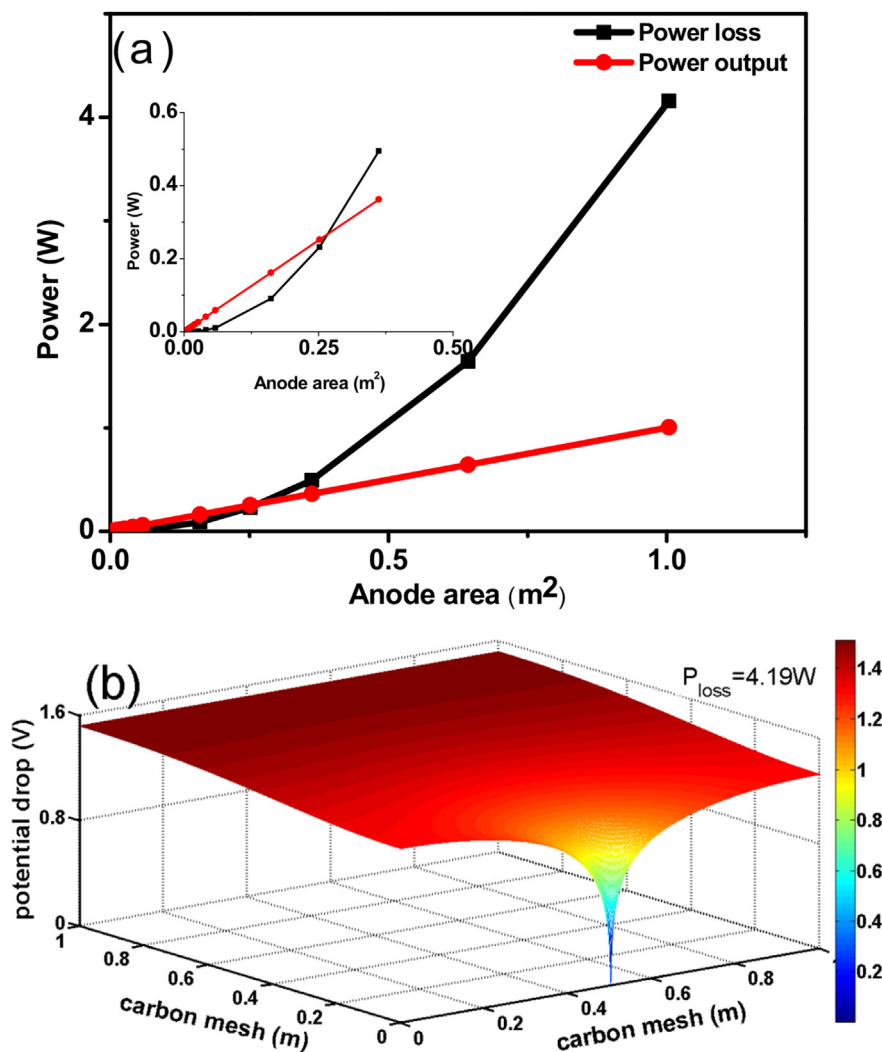


Fig. 3. Power output ideally enlarged from power density 1 W m^{-2} (without accounting in factors affecting power density) and power loss of MFC as a function of anode area (a). Inset, the power output and power loss in the region of small anode area; potential drop distribution of the 1 m^2 carbon mesh (b).

leading-out terminal to 2 points (CP-2) increased the power by 21.4% to $46.5 \pm 1.7 \text{ mW}$. Further increasing leading-out terminal to 5 points (CP-3) resulted in the power increasing by 27.8% to $48.9 \pm 2.1 \text{ mW}$. Those power increases were due to the reduction in the anode ohmic resistance by adding leading-out points. Those results demonstrated that the anode ohmic resistance in large-scale MFC had a serious constrain on power output. Besides, the current density corresponding with the maximum power output tended to be lower as anode ohmic resistance increased, which was consistent with the simulation results.

At the current density of 1 A m^{-2} , the power losses for three connection patterns were calculated as 18.2 mW (CP-1), 6.4 mW (CP-2), and 3.4 mW (CP-3) (Table 1), while the corresponding power generations were 32.4 mW, 45.0 mW, 48.1 mW respectively. However, the sum of the power loss and power generation for each of the three different configurations was around 51 mW, which indicated that the power generation was only influenced by the leading-out terminal configuration in this case. The power loss under CP-1 accounted for as high as 36.0% to the sum of the power generation and loss. This proportion decreased to 6.6% under CP-3. Those results showed that our simulation well corresponded with the experiment.

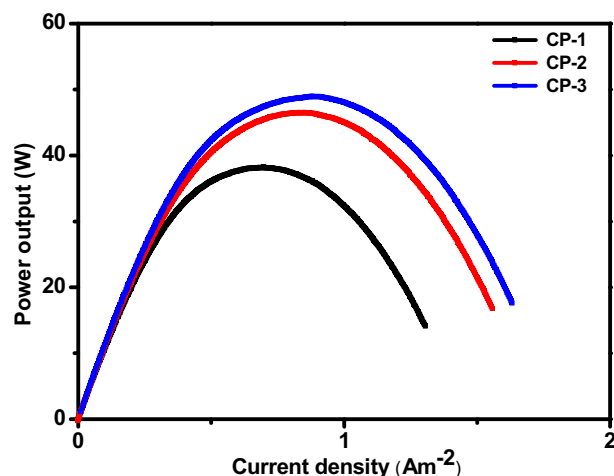


Fig. 4. Power output as a function of current density with different connecting patterns in the SC-MFC.

Table 1The power loss, power generation for the SC-MFC under CP-1, -2, -3 at 1 A m^{-2} .

Connecting pattern	CP-1	CP-2	CP-3
Power loss calculated (mW)	18.2	6.4	3.4
Power generation measured (mW)	32.4	45.0	48.1
The sum of power generation and power loss (mW)	50.6	51.4	51.5

In order to further illustrate the effect of the anode leading-out terminal on power output of MFC at high current density, a virtual MFC was supposed by combining the anode from a large-scale (the DC-MFC) MFC and the cathode from a small-scale MFC. Linear Fitting ($R^2 > 0.99$) was done for both the anode polarization curves in the DC-MFC (Fig. 5(a)) and the cathode polarization curve in the small-scale MFC (Fig. 5(b)). The power density of the virtual MFC under same configuration could be calculated based on the fitting results. In this approach, the effects of the cathode performance on the power generation could be considered as completely eliminated during scaling up. The anode polarization resistance of the DC-MFC (calculated from the slope of fitting line) was 0.44Ω for CP-3, which was 51.5% of that under CP-1 (0.85Ω) (Fig. 5(a)). Increasing by 56.2% from the power density of the virtual MFC under CP-1 (276.1 mW m^{-2}), the power density under CP-3 reached 431.2 mW m^{-2} (Fig. 5(c)). However, the power density under CP-3 was only 62.0% of the counterpart in small-scale MFC (696.4 mW m^{-2}), which indicated the existence of other factors other than anode ohmic resistance for losing 38.0% of the power during scaling up. In order to compare the simulation with the experiment results from the virtual MFC, the simulated power density curves were calculated based on subtracting or adding the power loss difference from the power density curve under CP-3 (Fig. 5(c)). There was little difference between simulated and experiment results with respective deviation of 10.9% and 6.3% for CP-1 and CP-2 in terms of the maximum power density. It again confirmed that our simulation work well corresponded to our experiment. The deviation might come from our assumptions, such as negligible contact resistance, even distribution of microbes and current input. Without the power loss caused by the anode ohmic resistance, the maximal possible power density of the virtual MFC was estimated as 474.1 mW m^{-2} .

3.3. Methods for reducing power loss

The only two ways to decrease power loss were to reduce ohmic resistance on anode and adjust current flows. Therefore, two measures could be taken as to, 1. alter leading-out terminal configuration; 2. change anode material from carbon material to metal with low resistivity.

For the first approach, the distance between the spot where electron generates and leading-out terminal should be shortened. The distribution of potential drop and the power loss in different leading-out terminal configurations on the 1 m^2 carbon mesh were simulated (Fig. 6). All the connecting configurations bore less power loss than that with one point leading out. Of all the configurations, the power loss of the configuration (f) was the lowest (0.04 W), and was only 2.4% of the configuration (a) which was very common in large-scale MFCs. Adding two strips of metal, the power loss decreased by 82.9% from the configuration (b) to (c), and with similar efficiency (decrease by 41.7%) adding another strip from the configuration (c) to (d). With only one strip of metal belt, the power loss of the configuration (e) was only 24.3% of the configuration (b). So how to effectively utilize current collectors is of significance in large-scale MFC.

On the other hand, altering anode material lowered anode ohmic resistance so that less power loss would be caused by current flowing through the same distance. Calculating results showed that

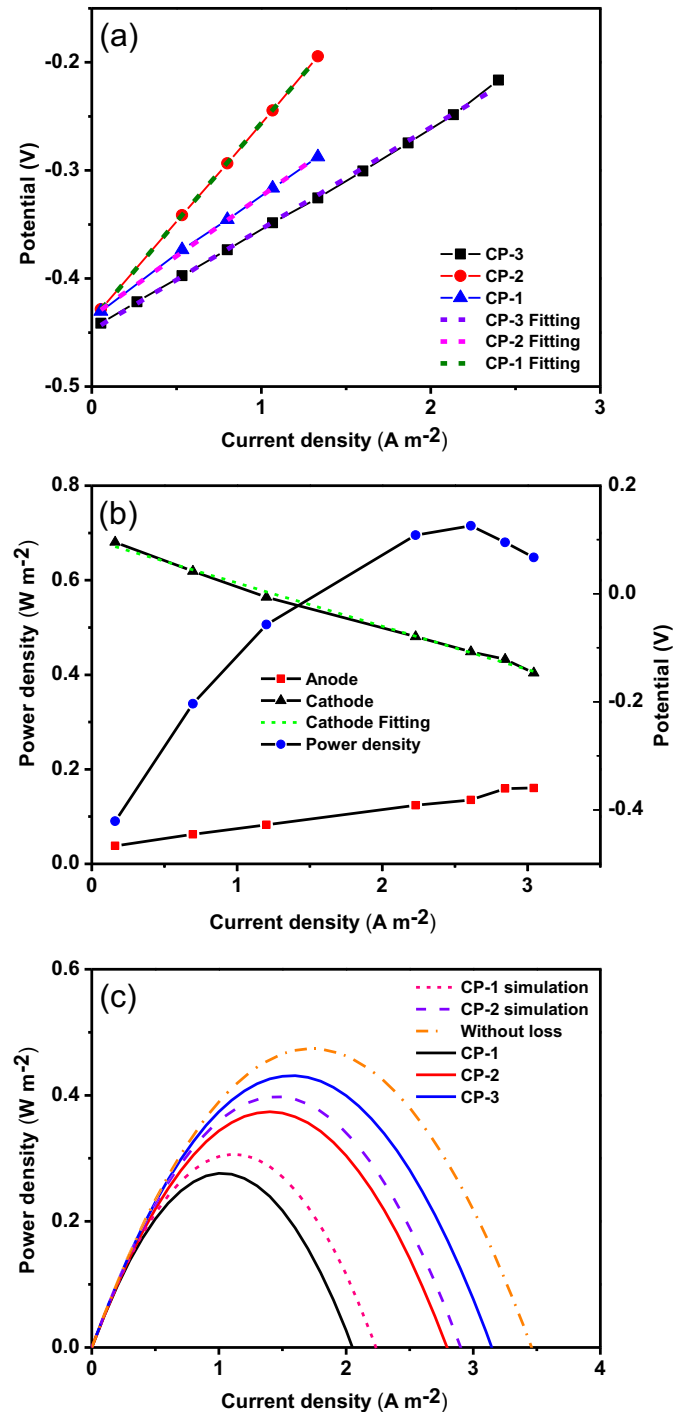


Fig. 5. Anode polarization curves and their fitting curves in the DC-MFC (a); power and polarization curves in the small-scale MFC (b); power density as a function of current density under different connecting patterns for the virtual MFC and correlated simulation results (c).

potential drops for the most part of the stainless steel and brass mesh anode were low even with one leading-out point (Fig. 7). The power loss with the two types of metal mesh was only 2.7% and 0.3% of that with the carbon mesh anode. The power losses corresponded with resistivity difference. Moreover, the power loss of brass mesh was only 27.5% of that of carbon mesh under the configuration (f).

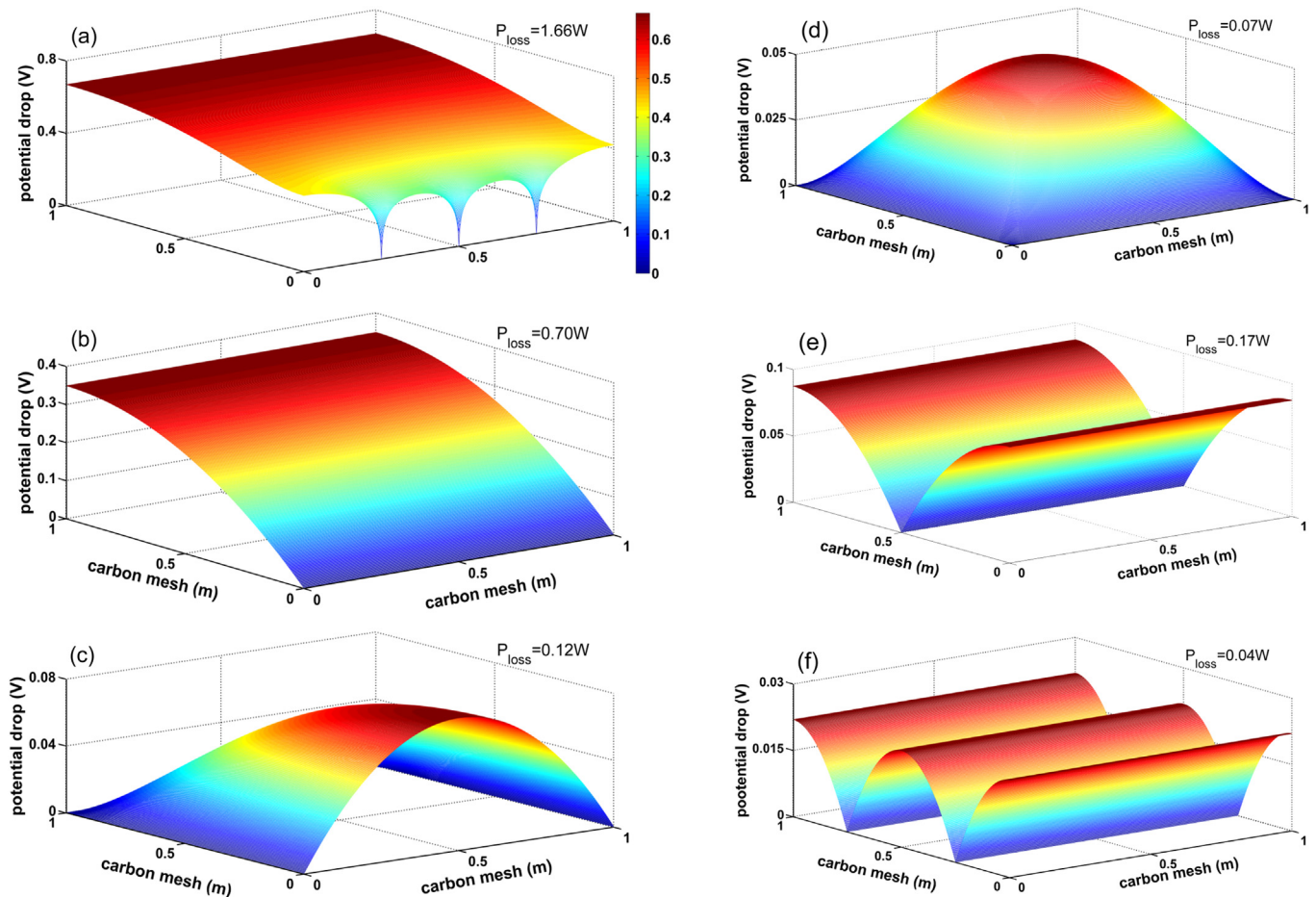


Fig. 6. Potential drop distribution and power loss of different leading-out terminal configuration. (a) Three nodes from one side; (b) all nodes in one side; (c) all nodes from three sides; (d) all nodes from four sides; (e) all nodes from axis line; (f) all nodes from two 1/4 axes.

4. Discussion

4.1. Effects of anode ohmic resistance on large-scale MFC

For the small-scale MFC, the power loss brought by the anode resistance increases from 0.54 mW m^{-2} to 6.88 mW m^{-2} at 3 A m^{-2} when the anode enlarges from 4.84 cm^2 to 43.6 cm^2 , while the power density of a single-chamber air-cathode MFC with similar anode material can reach as high as 893 mW m^{-2} (3 A m^{-2}) [11]. The ratio of power loss to power output in small-scale MFC with an anode size smaller than 40 cm^2 is below 1%, indicating that the effect of the anode ohmic resistance may be overlooked in small-scale MFC.

Many reports show that the size of anode does have effect on the maximum power density of MFCs. When the anode surface area becomes larger than 50 cm^2 , power densities (normalized to the area) decrease to near 0, which was regarded as the reason of the well-known but not easily quantified factors, such as mass transport mechanism and electron transport mechanism [22]. This result fits well with our simulation on power loss and power output as the function of the anode area (Fig. 3). However, our results indicate that the low power output is highly related to the power loss caused by increasing anode ohmic resistance. Besides, high ohmic resistance at large anode will also influence both the electrons transfer from microbes to anode and distribution of microbes on anode surface, which will cause further decrease in power generation.

4.2. Reduction of power loss and potential drop on anode

With one point for leading out, common in small-scale MFC structure [11,15,20,27,28], the power loss can reach 4.19 W . Although the regular configuration (a) and (b) (Fig. 6) result in less power loss in some extent, the power losses are still as high as 1.66 W and 0.70 W at 3 A m^{-2} , which respectively equal to 185.7% and 78.1% of the power output obtained in the small-scale MFC [11]. The power loss can be decreased to 4.9% by adopting the configuration (f). The configuration (c), which has already been tested in an MFC [23], will result in a power loss of 83.2% if the anode is enlarged to 1 m^2 . Less power loss achieved by the configuration (f) indicates that large-scale anode should be divided into several parts for leading out.

Utilizing anode material with low resistivity, such as stainless steel mesh and brass mesh, can also efficiently reduce power loss by reducing anode resistance. Metal mesh is superior to carbon mesh in terms of power loss, but metal mesh is inferior in biocompatibility. Although there are some studies utilizing stainless steel as anode [27–29], large-scale anodes with high performance using metal mesh are needed to be developed.

The model developed here can be also used to improve the performance of the air cathode made with carbon cloth as current collector in scale-up MFC. Developing the appropriate leading-out configurations like graphite or metal plates used in other fuel cells will be needed for both anode and cathode in the large-scale MFC.

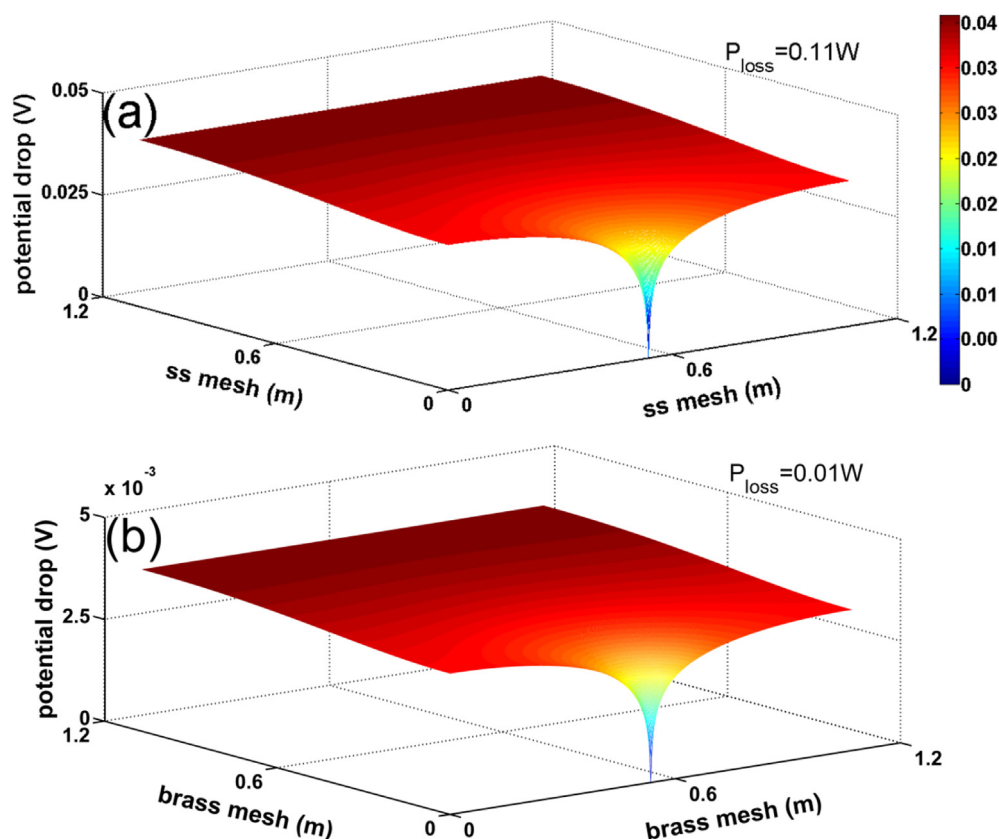


Fig. 7. Potential drop distribution and power loss of the 1 m^2 stainless steel mesh (a) and brass mesh (b) with one point leading out.

4.3. Other limiting factors

With the virtual MFC, the limiting factors for low performance of large-scale MFC can be identified. The power density goes down from 696.4 mW m^{-2} (the small-scale MFC) to 276.1 mW m^{-2} (the virtual MFC with one point leading out) when the anode size increased from 7 cm^2 to 2160 cm^2 , in which the power loss of 198.0 mW m^{-2} is due to bad leading-out terminal configuration and the other 222.3 mW m^{-2} is to the unknown reasons. Thus, the power loss caused by bad leading-out terminals accounts 47.1% of the total power loss. Though unknown loss hasn't been well understood, what can be confirmed is that the loss comes mainly from anode. The overpotential of anode in the DC-MFC under CP-3 was still greater than that in the small-scale MFC at the same current density (Fig. 5), which indicates the inferior anode performance of the large-scale MFC. The possible inhomogeneous biofilm grown on anode may be partially responsible for the low performance of anode. Therefore, further researches on the unknown loss should be carried on.

5. Conclusions

A simple model for calculating power loss of anode resistance was setup and verified by experiment. The results showed that the anode resistance, which has been overlooked, is one of the limitations for high performance of large-scale MFCs. The power loss of 1 m^2 carbon mesh could be as high as 4.19 W (3 A m^{-2}). Due to this kind of power loss, the power density of MFCs decreased by 21.7% for the SC-MFC. The power loss brought by anode ohmic resistance could account for as much as 47.1% of total difference in the power density between the small-scale and large-scale MFC. Reducing power loss by changing connecting configuration and altering

anode material can effectively decrease the power loss to 0.04 W and 0.01 W respectively. Great attention should be paid to the ohmic resistance of anode for scale-up MFC to obtain high performance.

Acknowledgments

Authors acknowledge the support from the National Natural Science Foundation of China (no. 21073163, no. 51278448), the National High Technology Research and Development Program of China (863 Program) (no. 2011AA060907), and Zhejiang Provincial Natural Science Foundation, China (no. Z4110186). Yaoli Ye acknowledges Dr. Dan Sun for the useful suggestions on the paper organization.

References

- [1] K. Rabaey, P. Clauwaert, P. Aelterman, W. Verstraete, *Environ. Sci. Technol.* 39 (2005) 8077–8082.
- [2] B. Min, B.E. Logan, *Environ. Sci. Technol.* 38 (2004) 5809–5814.
- [3] Z. He, S.D. Minteer, L.T. Angenent, *Environ. Sci. Technol.* 39 (2005) 5262–5267.
- [4] F. Zhu, W. Wang, X. Zhang, G. Tao, *Bioresour. Technol.* 102 (2011) 7324–7328.
- [5] H. Liu, B.E. Logan, *Environ. Sci. Technol.* 38 (2004) 4040–4046.
- [6] Y.Z. Fan, H.Q. Hu, H. Liu, *J. Power Sources* 171 (2007) 348–354.
- [7] B.Y. Jia, D.W. Hu, B.Z. Xie, K. Dong, H. Liu, *Biosens. Bioelectron.* 41 (2013) 894–897.
- [8] Y. Fan, E. Sharbrough, H. Liu, *Environ. Sci. Technol.* 42 (2008) 8101–8107.
- [9] G.-C. Gil, I.-S. Chang, B.H. Kim, M. Kim, J.-K. Jang, H.S. Park, H.J. Kim, *Biosens. Bioelectron.* 18 (2003) 327–334.
- [10] B. Logan, S. Cheng, V. Watson, G. Estadt, *Environ. Sci. Technol.* 41 (2007) 3341–3346.
- [11] X. Wang, S. Cheng, Y. Feng, M.D. Merrill, T. Saito, B.E. Logan, *Environ. Sci. Technol.* 43 (2009) 6870–6874.
- [12] S. Tanisho, N. Kamiya, N. Wakao, *J. Electroanal. Chem. Interfacial Electrochem.* 275 (1989) 25–32.
- [13] Y. Fan, H. Hu, H. Liu, *Environ. Sci. Technol.* 41 (2007) 8154–8158.

- [14] L. Zhuang, Y. Yuan, Y. Wang, S. Zhou, *Bioresour. Technol.* 123 (2012) 406–412.
- [15] H. Liu, S. Cheng, L. Huang, B.E. Logan, *J. Power Sources* 179 (2008) 274–279.
- [16] Z. Li, L. Yao, L. Kong, H. Liu, *Bioresour. Technol.* 99 (2008) 1650–1655.
- [17] I.S. Kim, K.-J. Chae, M.-J. Choi, W. Verstraete, *Environ. Eng. Res.* 13 (2008) 51–65.
- [18] A.J. Hutchinson, J.C. Tokash, B.E. Logan, *J. Power Sources* 196 (2011) 9213–9219.
- [19] R.A. Rozendal, H.V. Hamelers, C.J. Buisman, *Environ. Sci. Technol.* 40 (2006) 5206–5211.
- [20] H. Liu, S. Cheng, B.E. Logan, *Environ. Sci. Technol.* 39 (2005) 5488–5493.
- [21] S. Cheng, B.E. Logan, *Bioresour. Technol.* 102 (2011) 4468–4473.
- [22] A. Dewan, H. Beyenal, Z. Lewandowski, *Environ. Sci. Technol.* 42 (2008) 7643–7648.
- [23] Y.Z. Fan, S.K. Han, H. Liu, *Energy Environ. Sci.* 5 (2012) 8273–8280.
- [24] S. Cheng, J. Wu, *Bioelectrochemistry* 92 (2013) 22–26.
- [25] H. Liu, S. Cheng, B.E. Logan, *Environ. Sci. Technol.* 39 (2005) 658–662.
- [26] B.E. Logan, B. Hamelers, R. Rozendal, U. Schröder, J. Keller, S. Freguia, P. Aelterman, W. Verstraete, K. Rabaey, *Environ. Sci. Technol.* 40 (2006) 5181–5192.
- [27] X.H. Peng, H.B. Yu, X. Wang, N.S.J. Gao, L.J. Geng, L.N. Ai, *J. Power Sources* 223 (2013) 94–99.
- [28] X.H. Peng, H.B. Yu, X. Wang, Q.X. Zhou, S.J. Zhang, L.J. Geng, J.W. Sun, Z. Cai, *Bioresour. Technol.* 121 (2012) 450–453.
- [29] S. Tanisho, N. Kamiya, N. Wakao, *Bioelectrochem. Bioenergy* 21 (1989) 25–32.